Electronic Supplementary Material (ESI) for Journal of Materials Chemistry A.

Electronic Supplementary Information

Creating stable interfaces between reactive materials: Titanium nitride protects photoabsorber-catalyst interface in water-splitting photocathodes

Shinjae Hwang[1], Spencer H. Porter[1], Anders B. Laursen[1], Hongbin Yang[1], Mengjun Li[1], Viacheslav Manichev[1], Karin U. D. Calvinho[1], Voshadhi Amarasinghe[1], Martha Greenblatt[1], Eric Garfunkel[1]*, and G. Charles Dismukes[1,2]*

[1] Department of Chemistry & Chemical Biology, Rutgers, The State University of New Jersey, 610 Taylor Rd. Piscataway, NJ 08854.

[2] The Waksman Institute, Rutgers, The State University of New Jersey, 190 Frelinghuysen Rd, Piscataway, NJ 08854.

*Corresponding authors: egarf@chem.rutgers.edu, and dismukes@chem.rutgers.edu

Experimental details

Chemicals. Red P (98.9%, Alfa Aesar), Ni (99.99%, Aldrich), TiN target (99.5%, Kurt Lesker)

Reflectance measurement. All reflectance was measured with Xe arc lamp as a light source and collected by Andor Technology Shamrock SR303i-A imaging spectrometer equipped with Zeiss, Axio Vert.A1 microscope.

The reflectance (R) is plotted by:

$$R = (I_0R - I_b) / (I_0 - I_b)$$

where I_0 is reflected light source intensity from a silver mirror, I_b is background signals, and I_0R is reflected light intensity from the sample. Below 350 nm wavelength, background subtraction overcompensated the reflection signal due to the low incident light source intensity.

To conduct the wet condition measurement similar to a PEC operation condition, a quartz window (1mm thick) placed on the bottom and fixed the sample position 1 mm away from the quartz window to keep the water thickness constant during the measurements.

Pulsed laser deposition of TiN and TiO_2. For TiN deposition, Si (100) substrates were cleaned with acetone and deionized water followed by 5 min in Buffered Oxide Etch (BOE) 6:1vol. NH_4F/HF prior to introduction into the PLD vacuum chamber. Pulsed laser deposition of TiN and TiO_2 were carried out using a KrF excimer laser Compex 205 ($\lambda = 248$ nm d = 7 cm, 10 Hz, 2.5 – 5 J cm^{-2}; Coherent). TiN deposition was carried out under high vacuum condition (5 – 7 × 10^{-4} Pa, 600 °C). For TiO_2, the chamber was pumped down to high vacuum (5 – 7 × 10^{-4} Pa), and deposition was carried out under oxygen partial pressure (P_{O2}: 6.7 Pa) at 300 °C

Thermal evaporation of nickel. To minimize native TiO_x ($x \leq 2$) formation on the TiN layer, a few seconds of BOE etching was performed on the TiN/Si electrode just prior to nickel deposition. Deposition of Ni was carried out at a rate of 1.0 Å/s as determined by quartz crystal microbalance (QCM).

RF sputtering of titanium. Si substrate was cleaned in the same manner as PLD deposition prior to introducing to the sputtering chamber. PVD 75 (Kurt J. Lesker) was used for the sputtering deposition. The chamber was pumped down to $2 – 3 \times 10^{-4}$ Pa and backfilled with Ar and kept at 1.1 Pa during deposition.

Chemical vapor phosphidation. A previous evacuated ($1 – 3 \times 10^{-3}$ Pa) and sealed quartz ampoule was heated in a furnace (500 °C, 3 h, +\–8 °C/min). In the ampule, red P (5mg) was loaded with a distance of 6 – 7 cm to the substrate, with bottleneck in-between ensuring the separation.

Faradaic Efficiency Measurement. Hydrogen was quantified on an automated online HP 5890 Series II GC (500 µL sample loop, series connected 6-inch packed HayeSep D + 6-inch packed MoleSieve 13X column, serial TCD + FID detectors, and N_2 carrier gas at 50 °C). The calibration curve was constructed from constant current electrolysis of water (0.5 M H_2SO_4 electrolyte) in a 3-compartment electrochemical cell using flame-annealed Pt foil as working electrode and IrO_x mesh as counter electrode, separated by a Nafion membrane. Hg/Hg_2SO_4 electrode is used for reference electrode. At steady state, samples of the headspace were taken (averaged, n = 3 at 10-minute intervals). The number of moles of H_2 is calculated using the following equation:

$$n_{H_2}(mol) = \frac{i \times t}{2F}$$

where i is the current in Amps, t is the time necessary to fill the sampling loop $(t = \frac{10\ ml}{min} \times \frac{1\ min}{60\ s} \times \frac{1}{0.5mL})$, and F is Faraday's constant. The calibration curve (area in the chromatogram as a function of hydrogen concentration) was constructed assuming 100% faradaic efficiency for water reduction on platinum at four three currents (linear fit, $R^2 = 0.999$). The faradaic efficiency of the HER for cubic-NiP_2 thin-film on Si and e-Si were measured in a similar fashion at different current (3 mA, and 5 mA, respectively). The value reported corresponds to the average ($n = 3$) of the headspace hydrogen concentration.

Sequential wet-etching process for uncovering Si solar cell. To protect the bottom Al contact during the etching process, a photoresist (AZ5214) was spin-coated on the back side of the wafer. To remove the Ag bus bar and underlying adhesion layer and Si_3N_4 coatings, Si solar cell wafers were dipped in HF/NH_4F mixture (1:6 buffer oxide etchant) for 30 min. This process will lift off the Ag contact by removing the Si_3N_4 layers and expose Al_2O_3. Al_2O_3 coating was removed by dipping in the concentrated H_3PO_4 at 40 C for 20 min with agitation. After a very short period (5s) of piranha solution, the remaining photoresist layer was removed with acetone. The etched Si solar cell wafer then washed with a copious amount of water and dried with N_2.

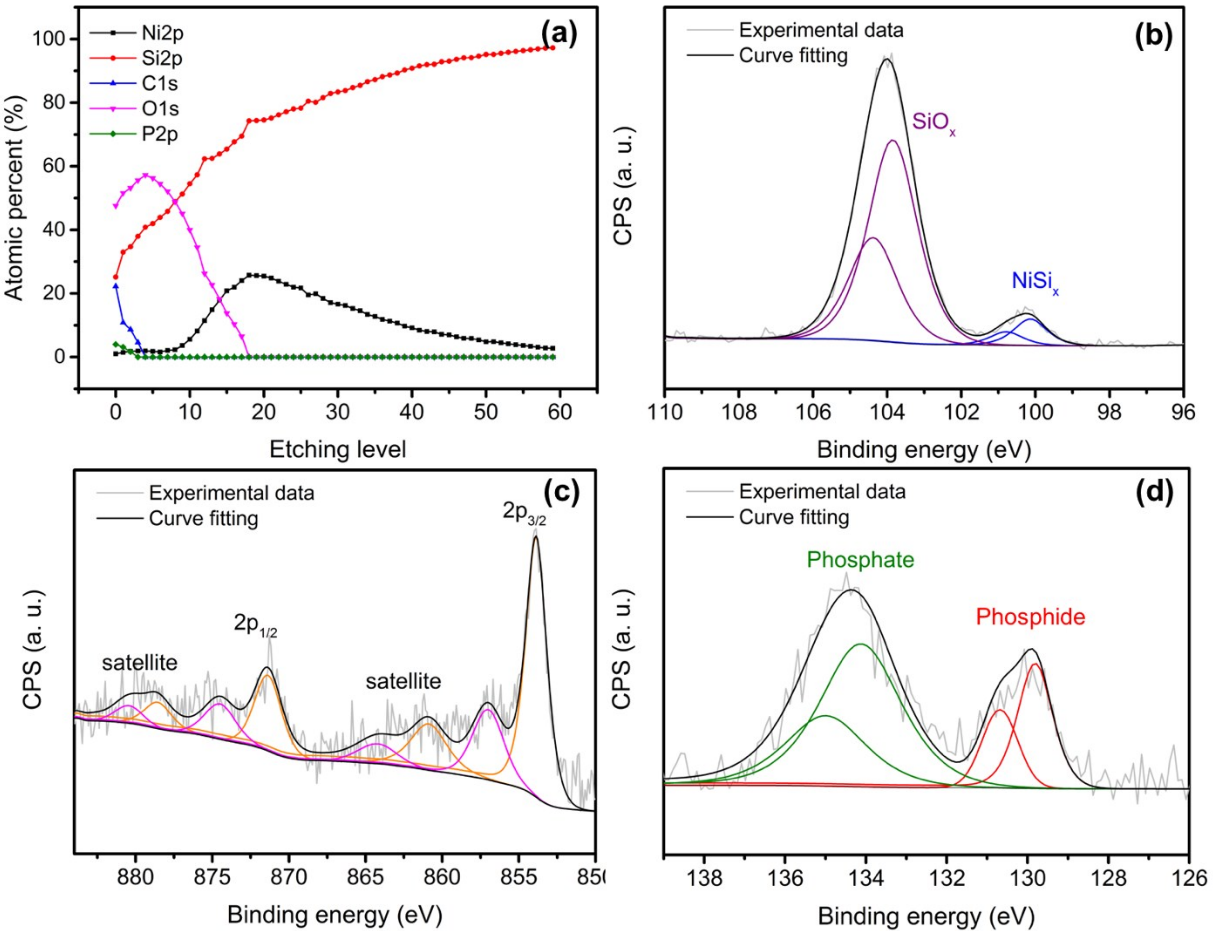

Figure S1. XPS analysis for a direct conversion of Ni to the nickel phosphide on a silicon substrate. The depth profile of the $NiP_x/NiSi_x/Si$ is shown in (a). Depth profiles indicate the majority of Ni was consumed to form nickel silicide with a phosphorus-containing surface layer. Si core level spectra (b) of the top layer demonstrates that the nickel silicide is exposed and forms a native oxide. Ni core level spectra (c) have metallic nickel ($NiSi_x/NiP_x$, purple) and NiO_x (orange) features. Similarly, P core level spectra (d) show nickel phosphide (red) and phosphate (green).

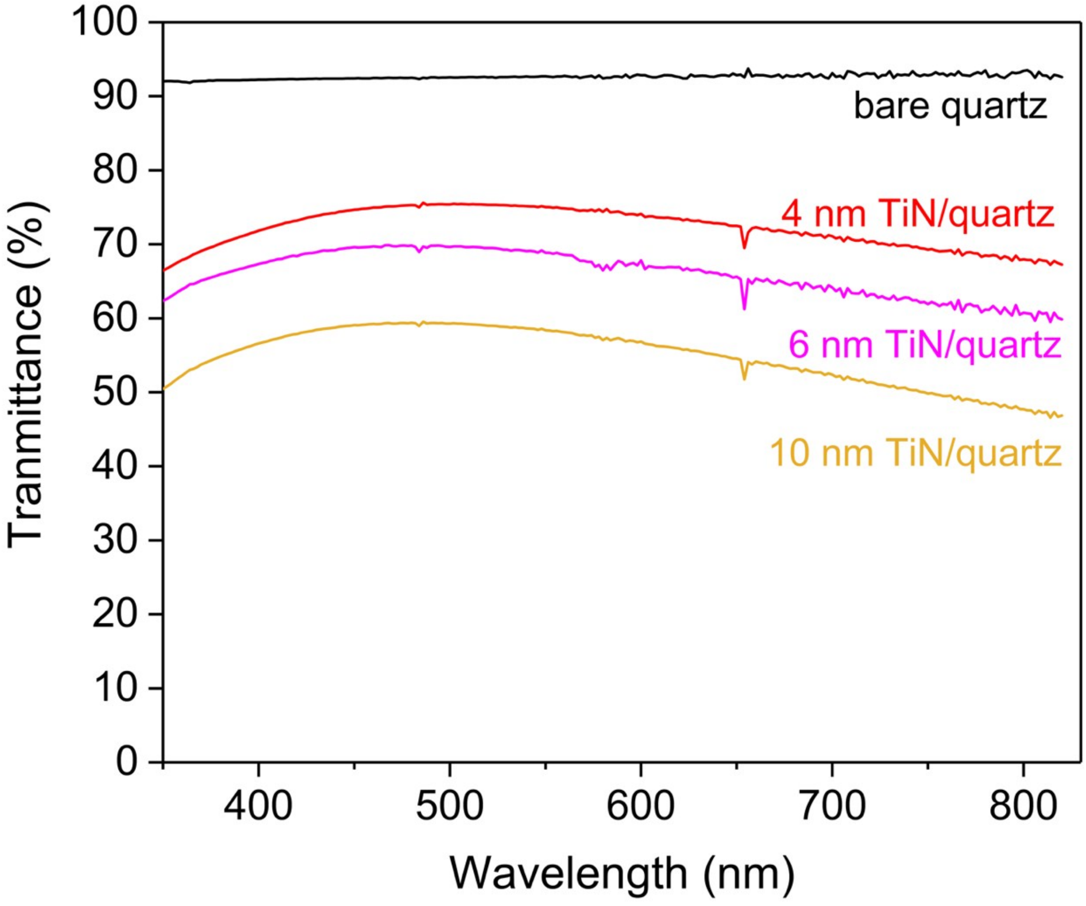

Figure S2. Transmittance spectrum of different thicknesses of TiN film deposited on a quartz substrate. The loss of transmittance from quartz substrate is due to the reflectance which also contributes to all other TiN coated samples.

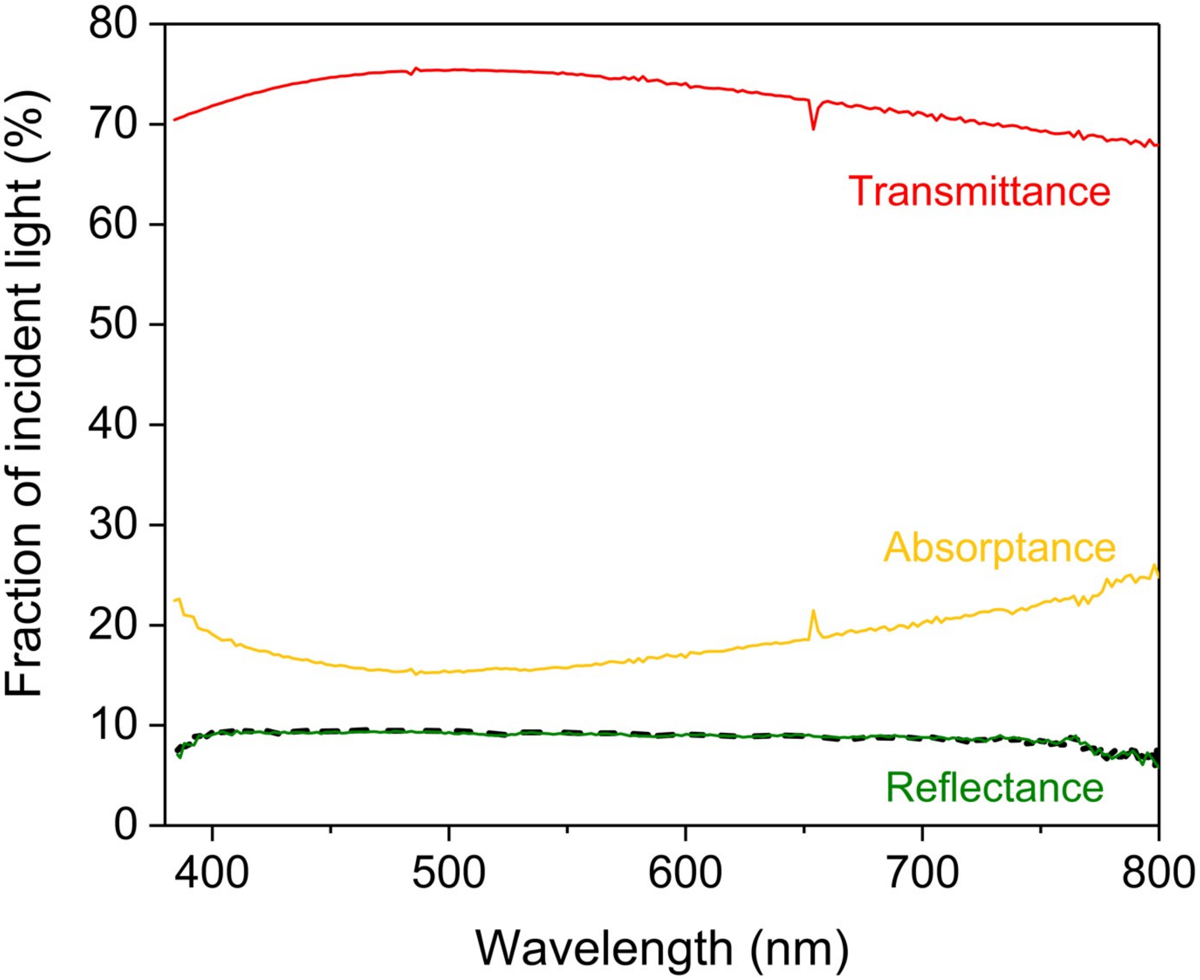

Figure S3. Optical transmittance, absorptance, and reflectance of 4 nm TiN coated on a quartz substrate. Since TiN layer is atomically smooth, scattering contribution is negligible. The black dash line is the reflectance of bare quartz which is the sum of contribution from top air/quartz and bottom quartz/air interfaces.

TiN film absorption coefficient estimation

To estimate absorption coefficient of the TiN film, we used general three-layer model shown here.

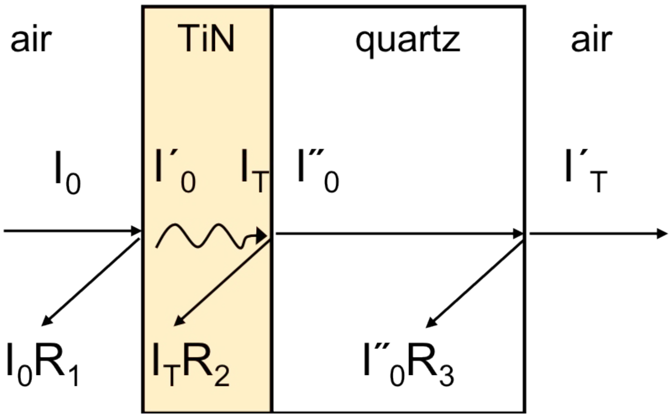

When the incident light intensity (I_0) propagate to the layers, the transmittance (T) can be defined

$$T = \frac{I_T^{'}}{I_0} = (1 - R_1)(1 - R_2)(1 - R_3)e^{-\alpha x}$$

Where R_i is reflectance of each interface, α is absorption coefficient, and x is thickness of TiN film (4 nm). Since the extinction coefficient of the quartz substrate is zero, there is no loss of the light intensity in the quartz medium. (no loss of I''_0 in quartz medium).

Because the difference between the total reflectance of TiN/quartz and bare quartz is negligible based on the Figure S3, we can estimate $R_1 \sim 0$, and $R_2 \approx R_3$ (same as quartz).

Then, absorption coefficient α is

$$\alpha = -\frac{1}{x} ln \frac{T}{(1 - R)^2}$$

At 500 nm, $$\alpha = -\frac{1}{(4 \times 10^{-9} m)} ln \frac{0.753}{(1 - 0.036)^2} = 5.2 \times 10^5\ cm^{-1}$$

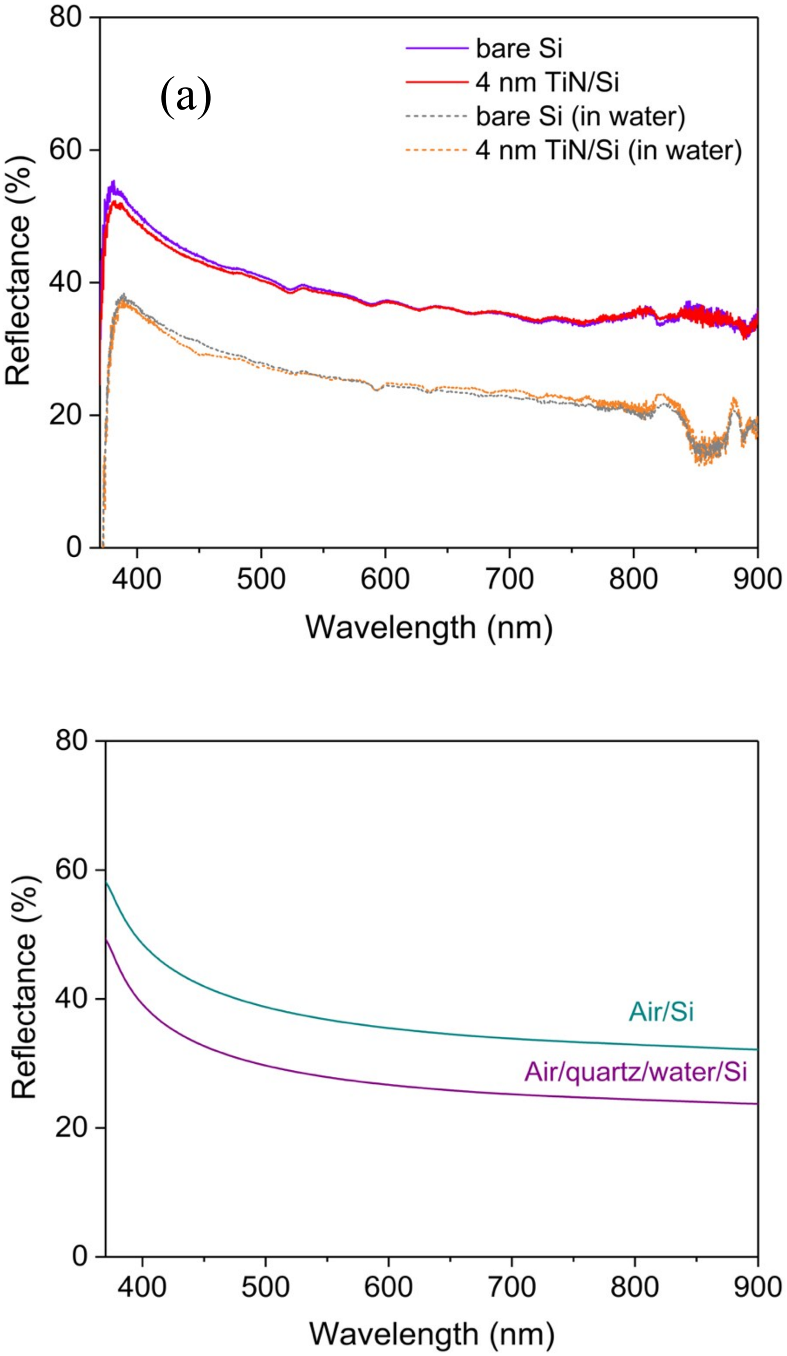

Figure S4. Reflectance of (a) bare Si and 4 nm TiN coated Si in air and with 1mm thick water layer. Calculated reflectance of air/Si vs. air/1mm quartz/1 mm water/Si based on the complex-m of Fresnel equations.[1] The small discrepancy between the experimental data and calculation might be attributed to the finite collection angle of objective lens during reflectance measurements and unconsidered Si conductivity in the calculation.

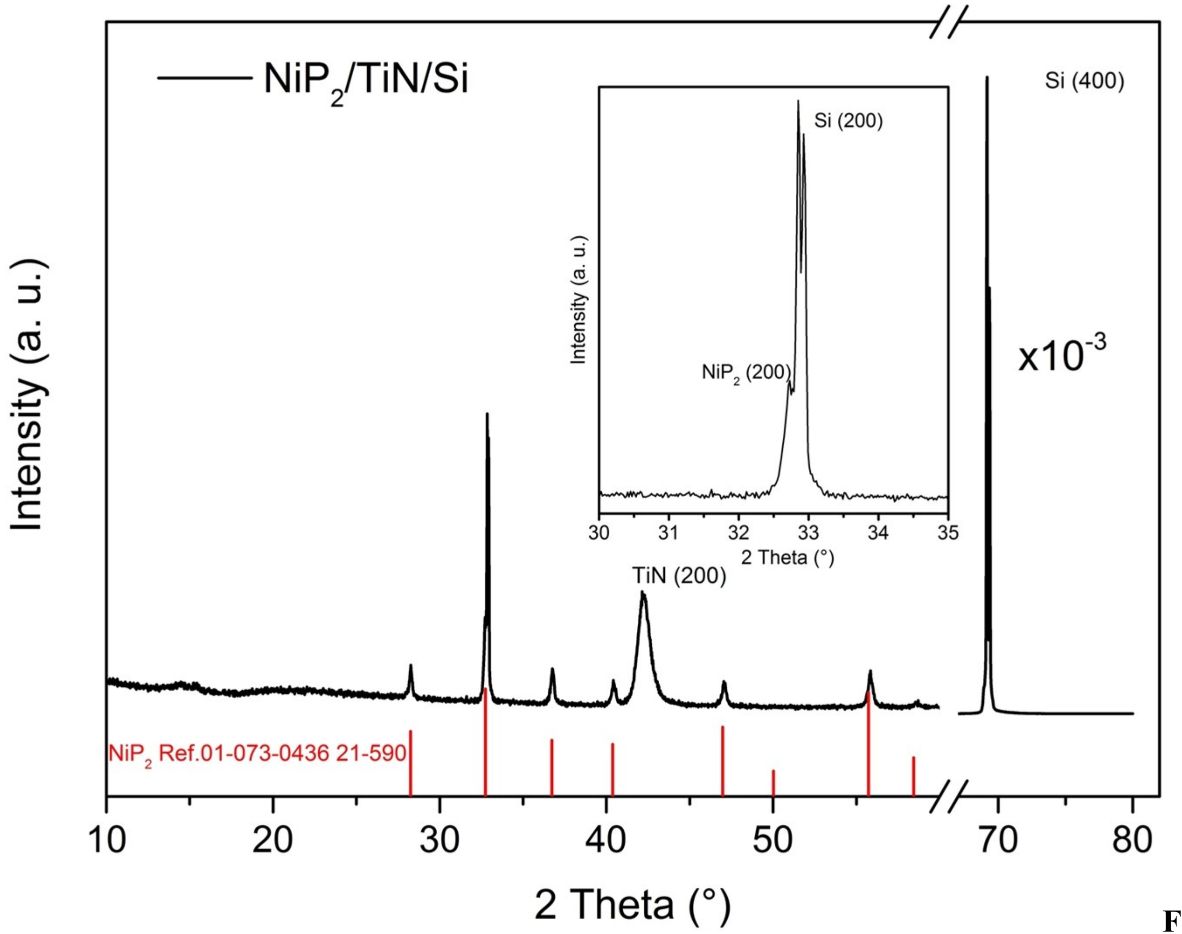

Figure S5. X-ray diffraction pattern of NiP$_2$/TiN/Si. 50 nm TiN was deposited by PLD on a fresh, BOE-etched Si substrate followed by a 150 nm Ni deposition, which was subsequently converted to NiP$_2$ though the P CVD step described in the main text. TiN only shows a reflection (200) at 42.2 °. A strong reflection of Si (200) and (400) are obtained at 32.8° and 69.1°, respectively. All other reflections are matched with the cubic NiP$_2$ reference, indicating our synthesis method forms phase-pure cubic NiP$_2$.

Rutherford backscattering (RBS) thickness estimation

Simulated RBS spectra give thickness information as the number of atoms per unit area (atoms/cm^2). Using the atomic density of each material, thickness can be estimated using the following formula:

$$Thickness = \frac{Atoms\ per\ square\ cm\ (\frac{atoms}{cm^2})}{Atomic\ density\ (\frac{atoms}{cm^3})}$$

Atomic density can be obtained using the following formula:

$$Atomic\ density = \frac{(Avogadro's\ number)(Density)}{Molecular\ weight/\#\ of\ atoms}$$

NiP_2 thickness:

The number of atoms per sq. cm of NiP_2 obtained from RBS is 4.0×10^{16} atoms/cm^2.

$$Thickness = \frac{(5.0\ \times 10^{16} atoms\ cm^{-2})}{(6.022\ \times 10^{23}\ mol^{-1})(4.89\frac{g}{cm^{-3}})(\frac{mol}{40.21\ g})}$$

$$= 6.82\ \times\ 10^{-7} cm$$

$$= 6.8\ nm$$

TiN thickness:

The number of atoms per sq. cm of the TiN obtained from RBS is 4.2×10^{16} atoms/cm^2. Although composition of the TiN was identified as $Ti_{0.39}N_{0.33}O_{0.27}$, we used the atomic density of TiN since oxygen incorporation would not significantly alter the atomic density.

$$Thickness = \frac{(4.2\ \times 10^{16} atoms\ cm^{-2})}{(6.022\ \times 10^{23}\ mol^{-1})(5.4\frac{g}{cm^{-3}})(\frac{mol}{30.93\ g})}$$

$$= 3.99\ \times\ 10^{-7} cm\ \approx 4.0\ nm$$

$Ni_{0.2}P_{0.39}Ti_{0.05}O_{0.18}N_{0.2}$ interfacial layer thickness:

The number of atoms per sq. cm of the interfacial layer obtained from RBS is 5.1 × 10^{16} atoms/cm^2. We used the density of $Ni_3(PO_4)_2$ for the calculation since this is the closest equivalent composition that exists in the literature.

$$Thickness = \frac{(5.1 \times 10^{16} atoms\ cm^{-2})}{(6.022 \times 10^{23}\ mol^{-1})(4.42 \frac{g}{cm^{-3}})(\frac{mol}{28.88\ g})}$$
$$= 5.53 \times 10^{-7} cm \approx 5.5\ nm$$

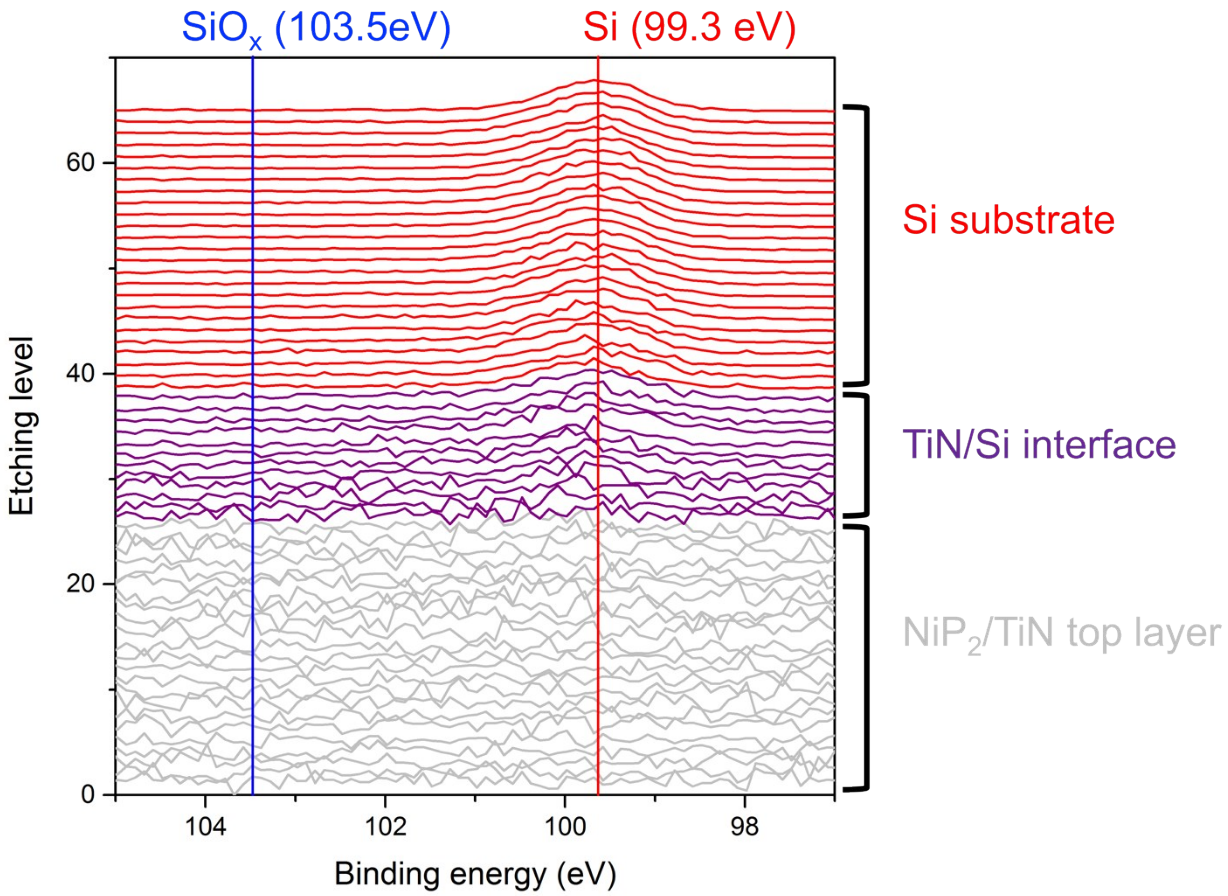

Figure S6. XPS depth profile of Si core level spectra on NiP$_2$/TiN/n$^+$p-Si photocathode. The intensity of all Si core level spectra was normalized to 1. From the top layer of NiP$_2$ to the TiN layer, no silicon signals are detected (gray). At the TiN/Si interface (purple), Si signals start to appear at 99.3 eV (red vertical line), which is corresponds to a Si substrate contribution. The Si signal becomes more pronounced as more layers are etched. During the profiling, SiO$_x$ signals were not observed (blue vertical line). It is worth noting that the selected Ar$^+$ sputtering condition etches the film at less than 1 nm/cycle, therefore it has adequate resolution to detect native oxide from silicon.

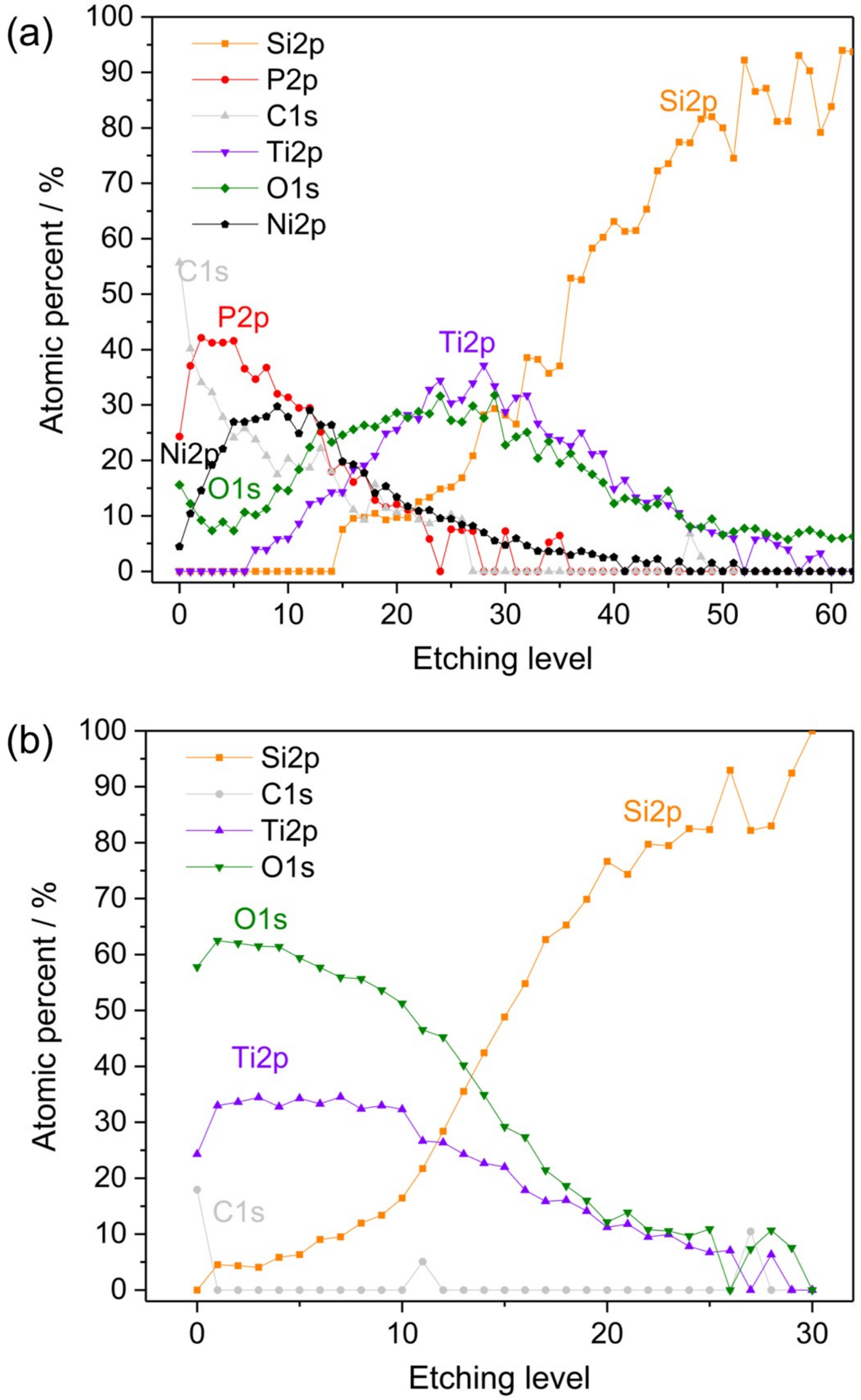

Figure S7. XPS depth profile of a) $NiP_2/TiO_2/Ti/n^+p$-Si and b) pristine $TiO_2/Ti/n^+p$-Si photocathode.

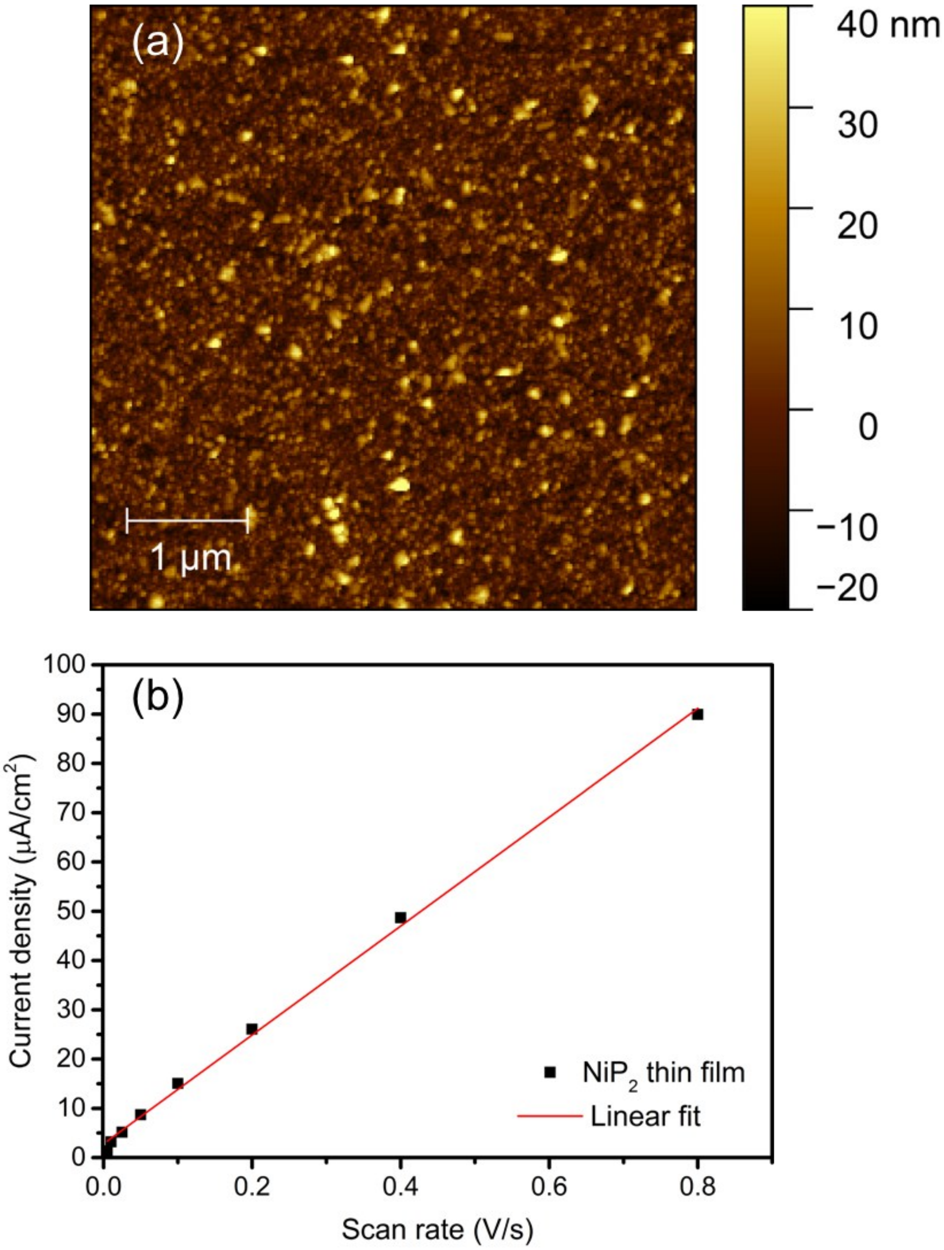

Figure S8. Determination of electrochemical surface area. A 5×5 µm atomic force microscope image **(a)** of $NiP_2/TiN/n^+Si$ shows a smooth film. The roughness factor is 1.08 $cm^2{}_{ECSA}/cm^2{}_{geo}$. The capacitive current as a function of scan rate **(b)** and the electrochemical capacitive currents were measured using cyclic voltammograms at 0.1 V vs. RHE where no faradaic processes occur. The intrinsic capacitance of the NiP_2 thin-film is 110 µF cm^{-2}. We assume 40 µF cm^{-2} as a flat surface, the same assumption used by Kibsgaard et al[2] allowing for direct comparison to literature values. Roughness factor from the intrinsic capacitance measurement is 2.75 $cm^2{}_{ECSA}/cm^2{}_{geo}$.

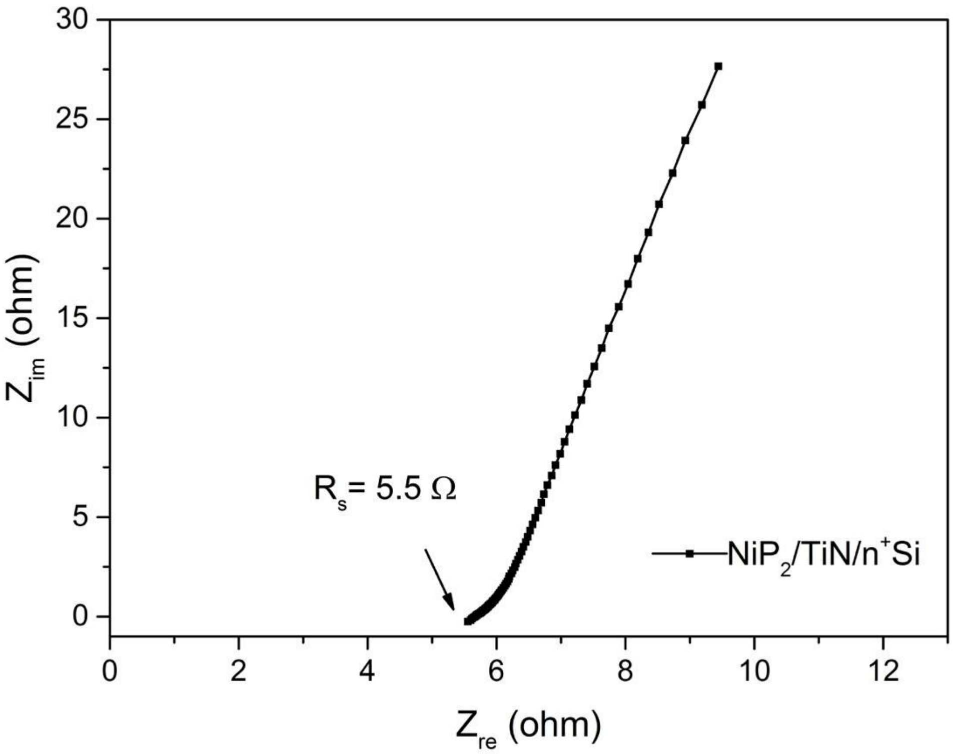

Figure S9. Electrochemical impedance spectroscopy (EIS) of the NiP_2 thin-film. Before each CV measurement, EIS was carried out to obtain the solution resistance (R_s), which is used for the *i*R correction. The average R_s obtained was 5.6 ± 0.6 Ω.

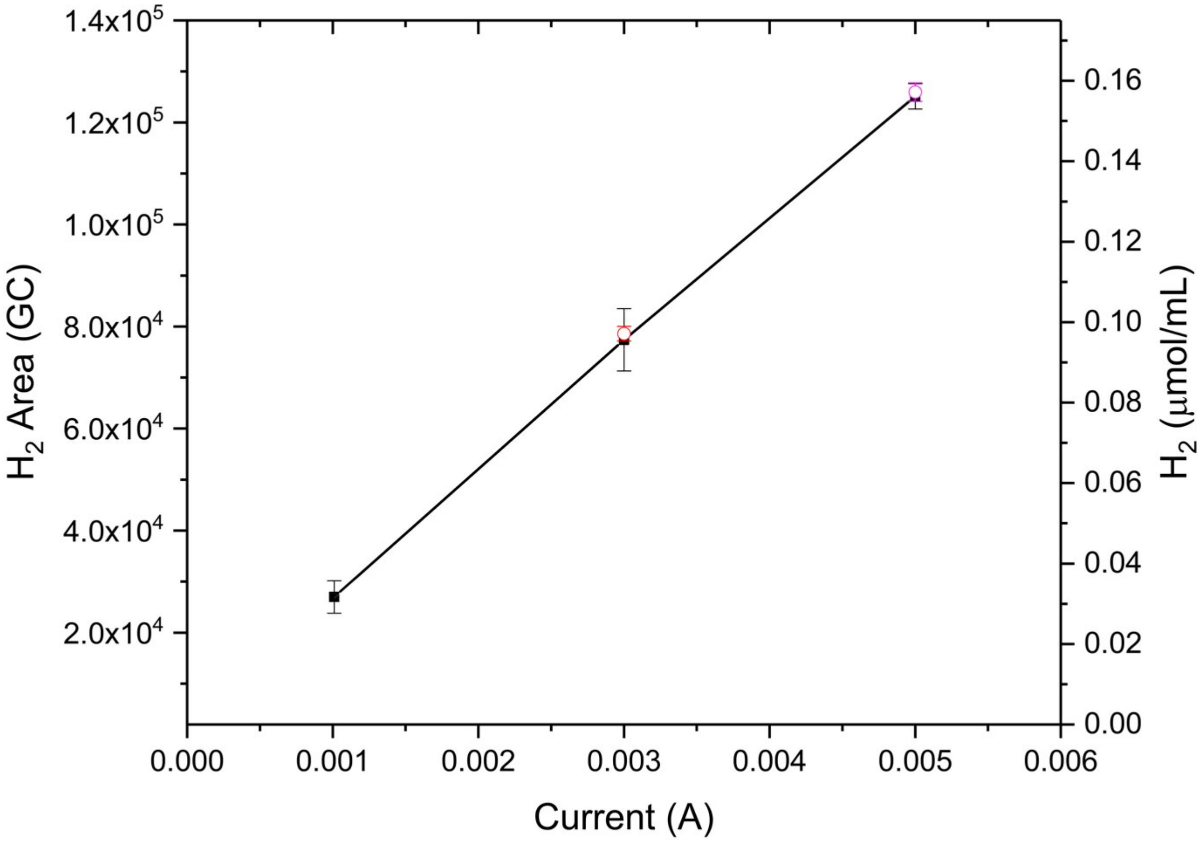

Figure S10. Faradaic efficiency test. The linear line is the calibration curve measured by the Pt foil benchmark. Red circle (○) and magenta circle (○) correspond to cubic-NiP_2/TiN layers on n^+-Si and e-Si, respectively. Both samples overlapped the Pt benchmark within the error bars.

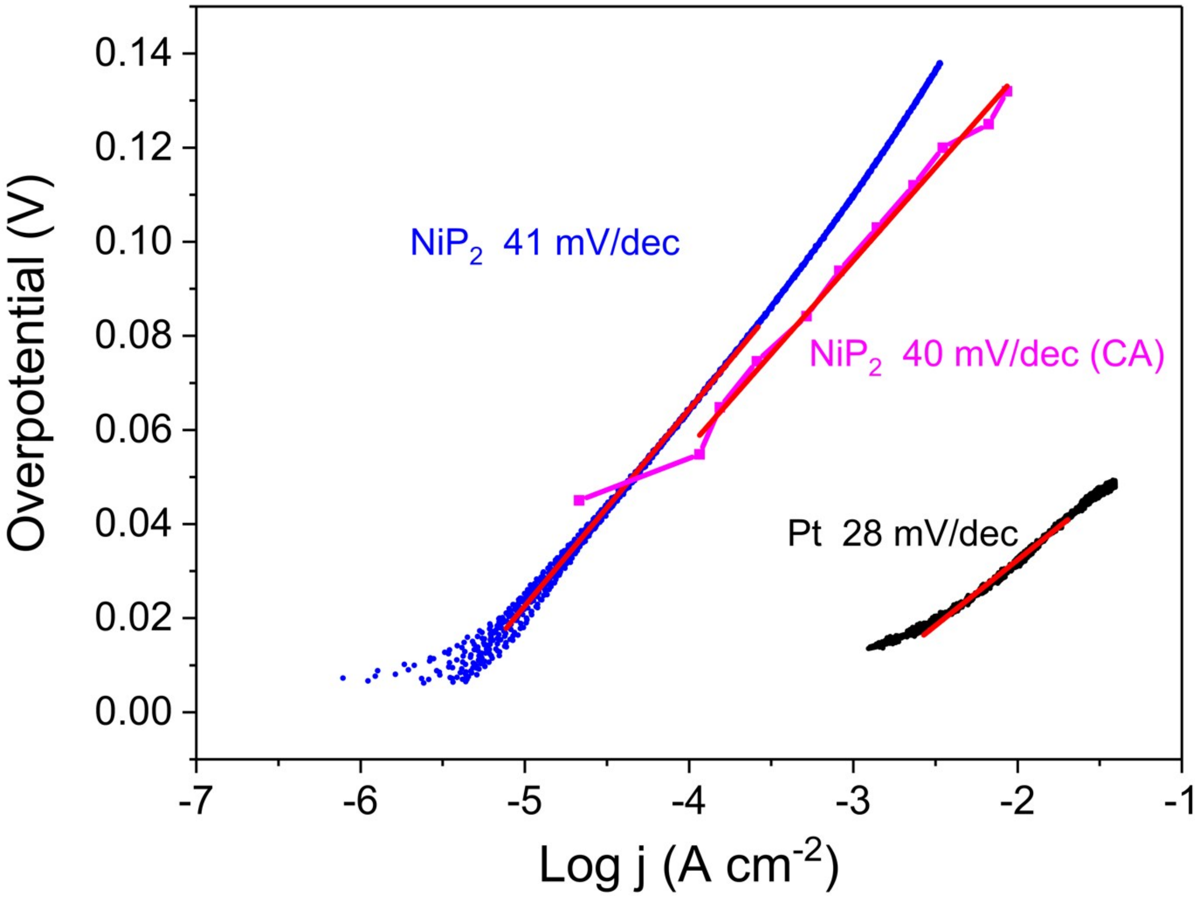

Figure S11. Tafel analysis of NiP_2 thin-film and polycrystalline Pt foil as a reference. The Tafel slope and the exchange current density of NiP_2 thin-film catalyst are 41 mV/dec and 3.0 $\times 10^{-6}$ A/cm$^2_{geo}$, respectively. The magenta curve corresponds to the Tafel slope of the NiP_2 thin-film catalyst measured by chronoamperometry at different fixed potentials. For reference, the Tafel slope and exchange current density of a polycrystalline Pt foil were also measured (28 mV/dec and 3.2 $\times 10^{-4}$ A/cm$^2_{geo}$, respectively).

Turn-over frequency (TOF) analysis

The turn-over frequency can be obtained using the following formula [2,3]:

$$TOF = \frac{\#\ total\ hydrogen\ turn\ overs/cm_{geo}^{2}}{\#\ surface\ sites/cm_{geo}^{2}}$$

In order to estimate the turn-over frequency of a catalyst as a function of overpotential, the number of surface active sites per surface area of our film needs to be determined. Since the exact active sites for hydrogen binding is unknown for cubic NiP_2, we employed the method used by Kibsgaard et al.[2] By using this method, the total number of surface sites from the unit cell of cubic NiP_2 crystal structure (PDF 01-073-0436) is used to estimate the average number of surface sites assuming all surface sites are active and then averaging these over the entire surface area of the unit cell. This gives a geometric average atom density per unit surface area.

Cubic NiP_2:

Cell volume: 163.72 Å^3 , 12 atoms per unit cell (4 Ni + 8 P)

$$\#\ surface\ sites = \left(\frac{12\ atoms/\ unit\ cell}{163.73\ \text{Å}^3}\right)^{\frac{2}{3}} = 1.75 \times 10^{15} atoms/cm_{ECSA}^{2}$$

To obtain the electrochemical surface area, we use the electrochemical intrinsic capacitance (EC) measurement. Using the cyclic voltammogram (Figure S4b) the roughness factor (R_f) is 2.75 $cm^2{}_{ECSA}/cm^2{}_{geo}$ while the atomic force microscope-derived R_f (Figure S4a) is 1.08 $cm^2{}_{ECSA}/cm^2{}_{geo}$. Using roughness factor from electrochemical surface area, the TOF can be calculated:

$$TOF = \left(j\frac{A}{cm^2}\right)\left(\frac{1\ mol}{96485.3\ C}\right)\left(\frac{1\ mol\ H_2}{2\ mol\ e^-}\right)\left(\frac{6.022\ \times 10^{23}\ H_2}{1\ mol\ H_2}\right)\left(\frac{1}{1.75 \times \frac{10^{15} atoms}{cm_{ECSA}^{2}} \times R_f}\right)$$

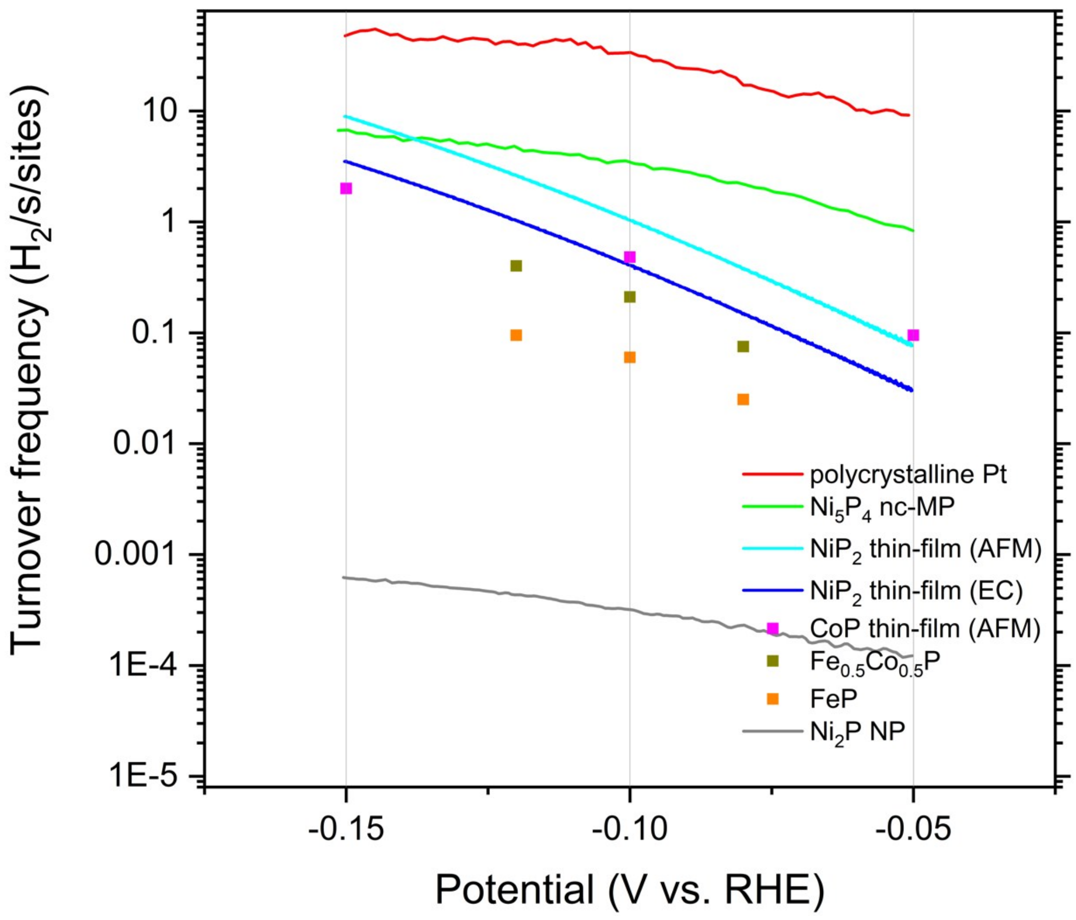

Figure S12. TOF comparison of selected transition metal phosphide and the NiP_2 thin-film. TOF of NiP_2 thin-film (EC) is calculated based on ECSA using the methods of Kibsgaard *et al.*[2] which used intrinsic capacitance for the determination of electrochemical surface area. For the comparison, TOFs (calculated using the same method described above) of the reported $Fe_{0.5}C_{0.5}P$ and FeP are shown. TOF of the NiP_2 thin-film (AFM) is calculated based on ECSA using the method reported by Hellestern *et al.*[3] A TOF of the CoP thin-film, calculated based on AFM, is also shown for comparison. Furthermore, other TMP catalysts (Ni_2P, Ni_5P_4) and Pt are included for reference. [4]

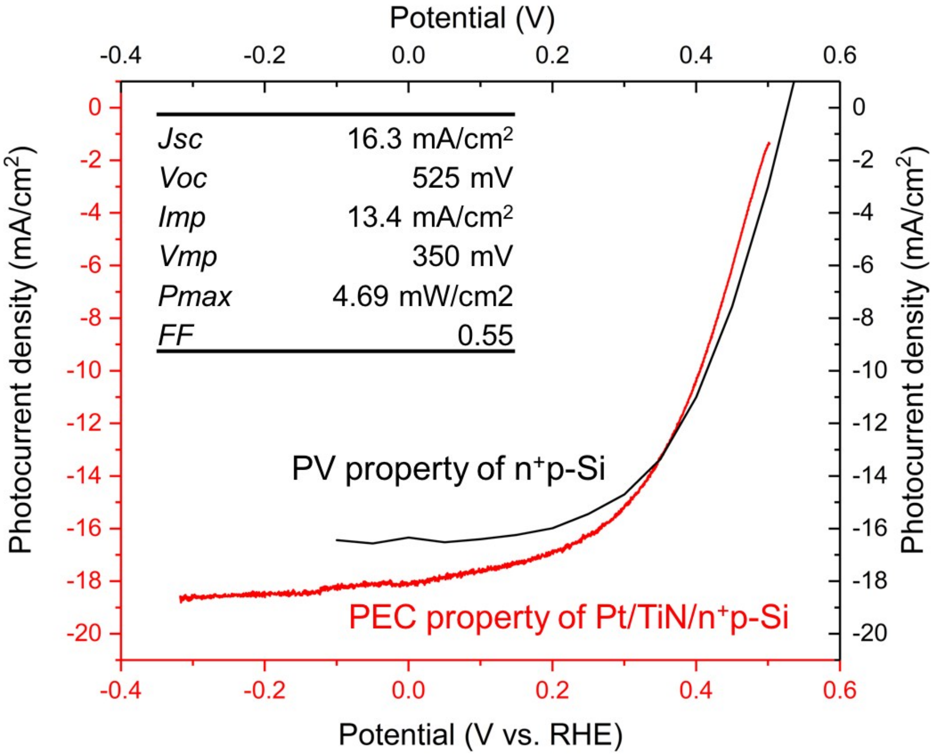

Figure S13. A comparison between the *J-V* curve of the as-prepared PEC (Pt/TiN/n$^+$p-Si, red) and PV (n$^+$p-Si, black). The inset is the calculated PV properties based on the measured J-V curve.

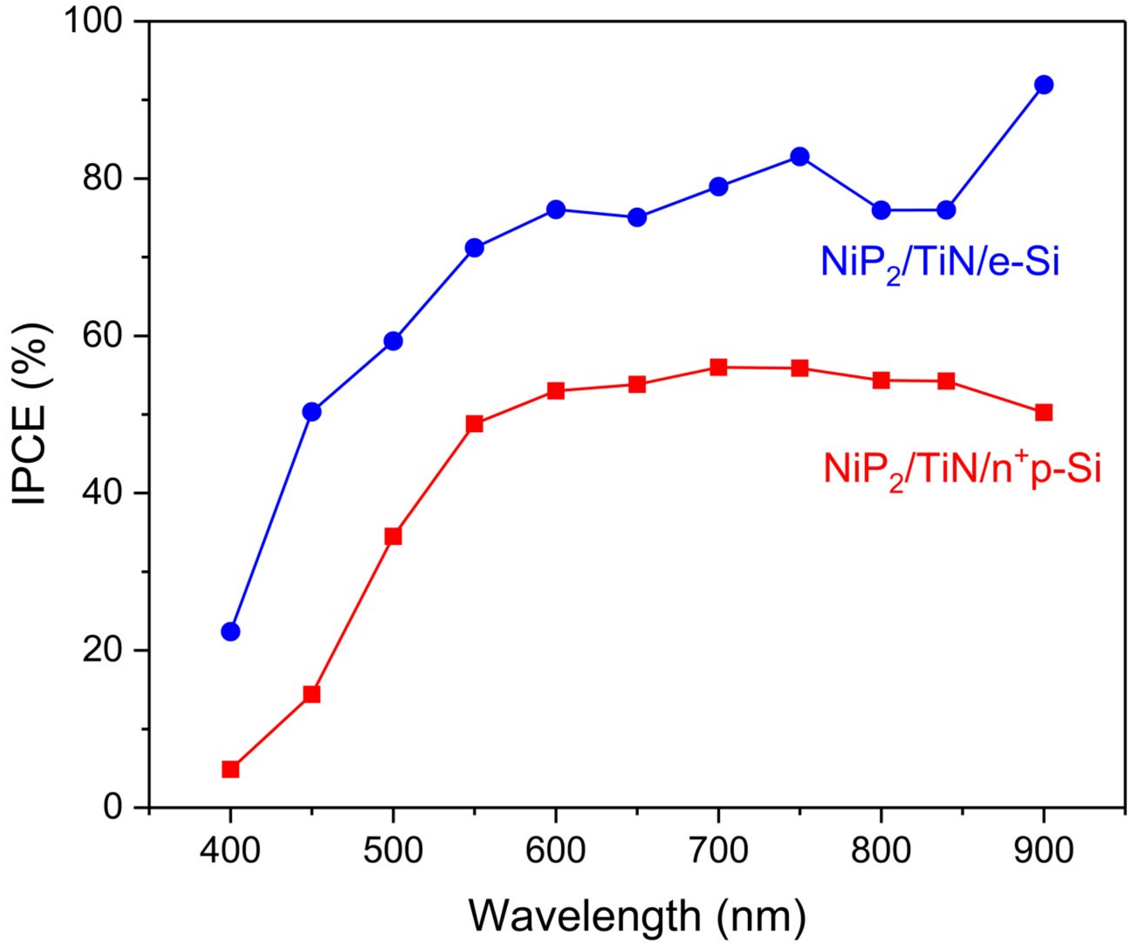

Figure S14. Incident photon-to-current efficiency (IPCE) of NiP$_2$/TiN/n$^+$p-Si and NiP$_2$/TiN/e-Si.

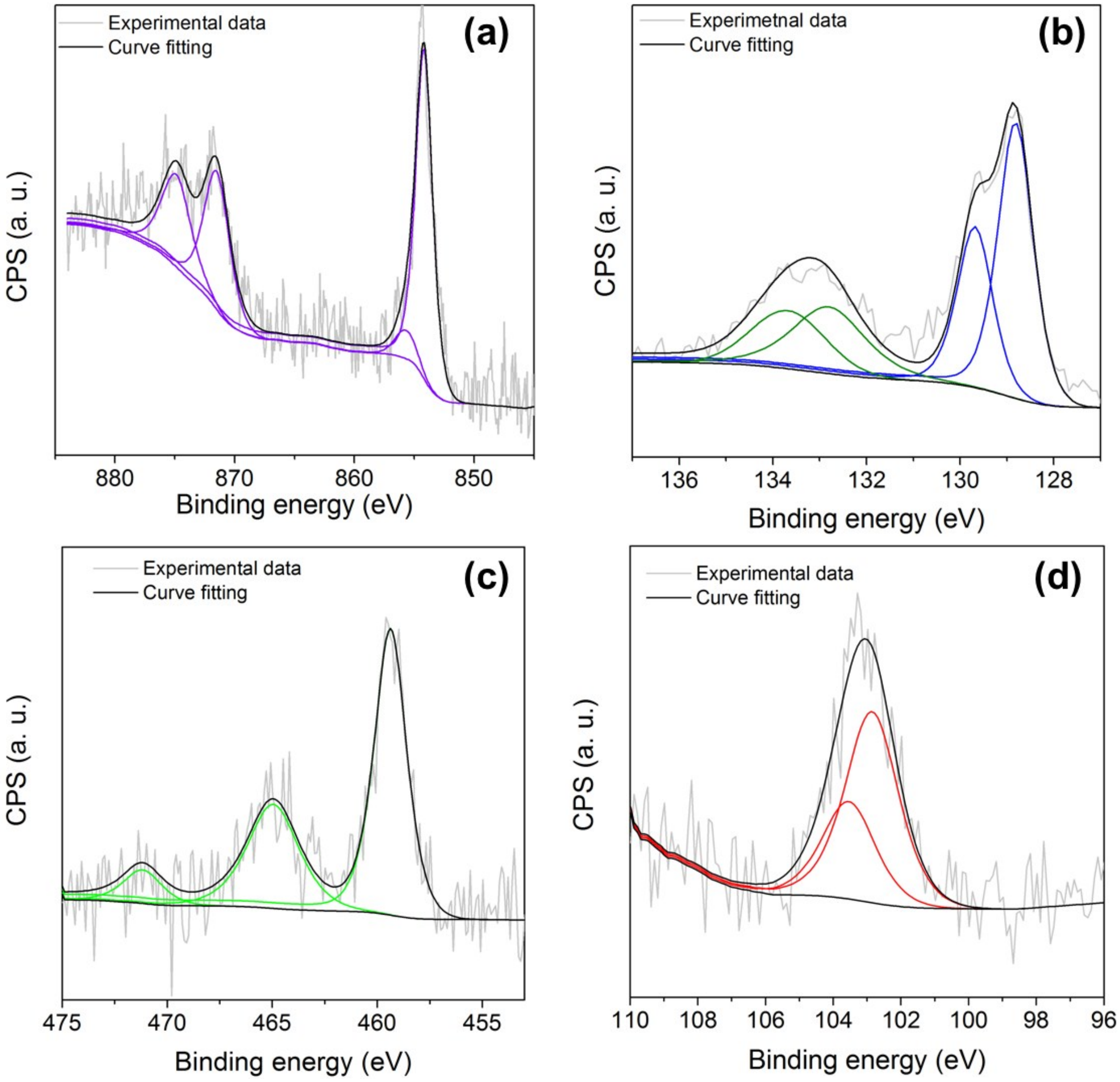

Figure S15. XPS top surface analysis of a NiP_2/TiN/n^+p-Si sample run for 125 hours. Binding energy of XPS spectra were selected at (a) Ni2p, (b) P2p, (c) Ti2p, and (d) Si2p core levels. The Ni2p spectra shows a metallic nickel feature of NiP_2 (violet). The P2p spectra has phosphide (blue) with small amount of phosphate (green). The Ti2p spectra exhibits a titanium oxide feature (binding energy of $2p^{3/2}$ is 458.8 eV),[5] and silicon oxide is also detected in the Si2p spectra (red)(binding energy of $2p^{3/2}$ is 103.2 eV). [6] However, gentle sputtering removed these peaks (Figure 6d) while the peaks associated with the top-layer of NiP_2 remains, which demonstrates that these are surface contaminants.

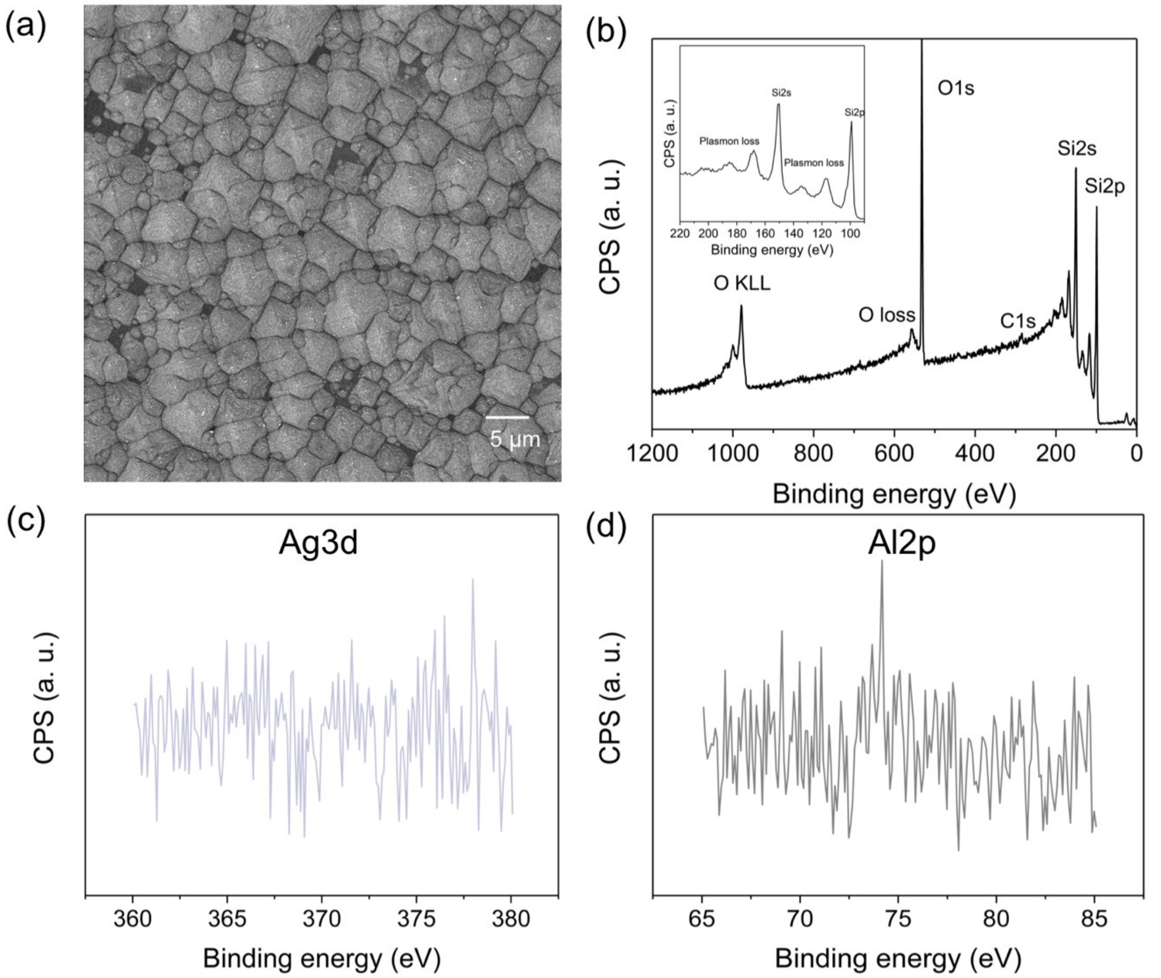

Figure S16. (a) Helium ion microscope image of sequentially etched Si solar cell substrate (e-Si). Inset shows plasmon loss peaks from Si2s and Si2p. X-ray photoelectron spectra of e-Si (b) survey (c) Ag3d core level, and (d) Al2p core level.

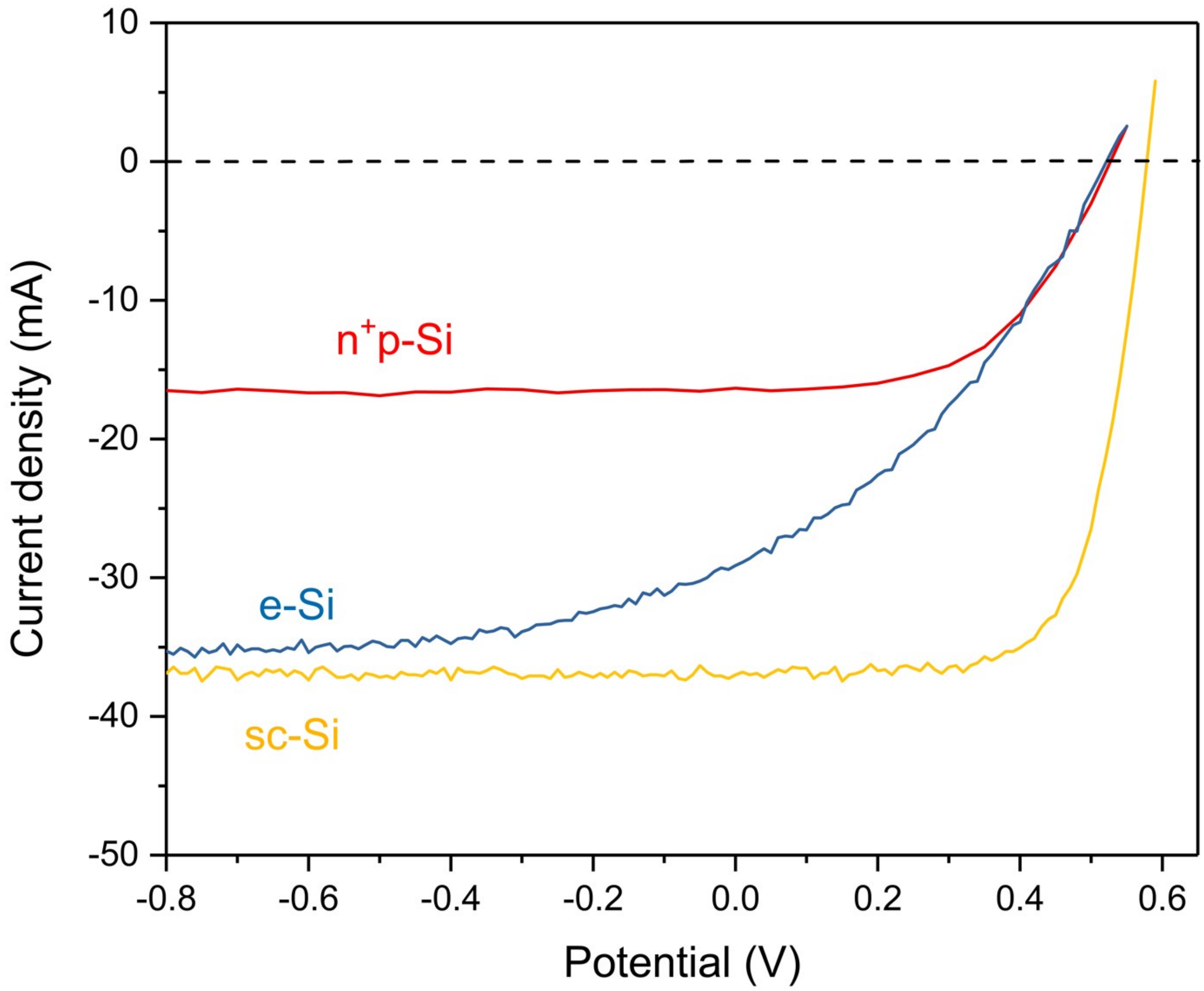

Figure S17. J-V curve of a different Si-based PV substrates.

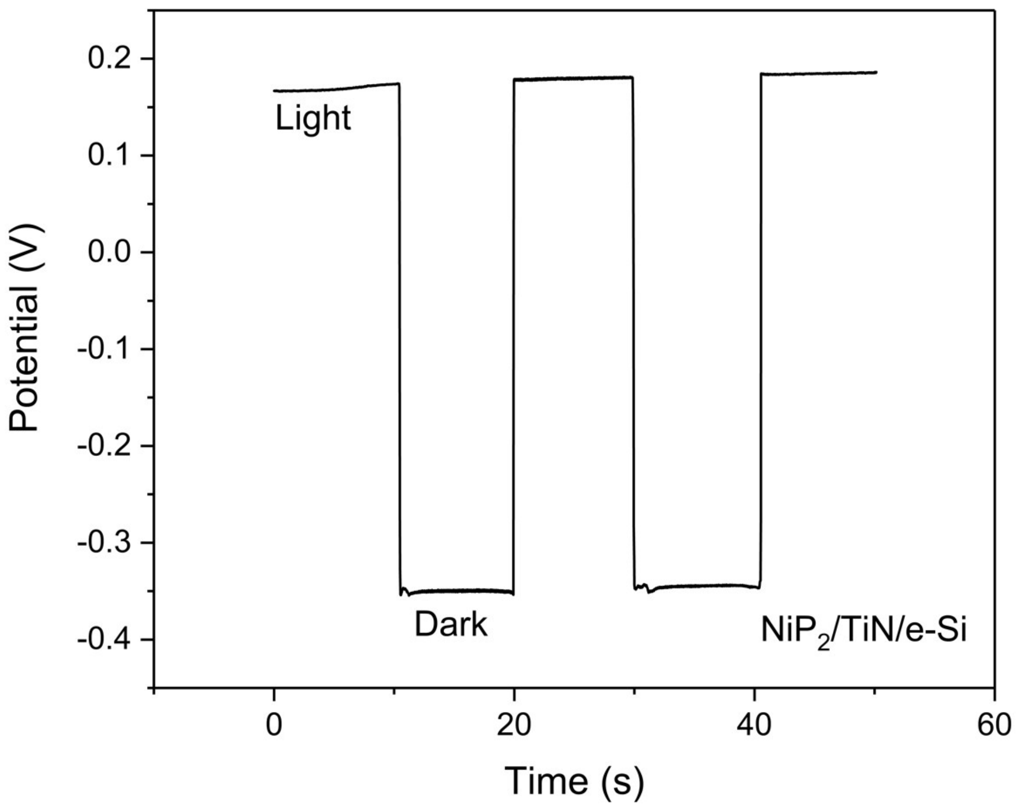

Figure S18. Open-circuit potential measurement under simulated AM 1.5 G illumination and dark for NiP_2/TiN/e-Si, V_{ph} is 520 mV

Table S1. Summary of PV properties for different Si-based PV substrates

	n^+p-Si	**e-Si**	**sc-Si**
J_{sc}	−16.3 mA/cm^2	−35.2 mA/cm^2	−37.3 mA/cm^2
V_{oc}	0.525 V	0.530 V	0.580 V
FF	0.55	0.22	0.67
Efficiency	4.69%	4.10%	14.29%

References

(1) FILMETRICS. Reflectance Calculator Https://www.Filmetrics.com/Reflectance-Calculator, 2018.

(2) Kibsgaard, J.; Tsai, C.; Chan, K.; Benck, J. D.; Nørskov, J. K.; Abild-Pedersen, F.; Jaramillo, T. F. Designing an Improved Transition Metal Phosphide Catalyst for Hydrogen Evolution Using Experimental and Theoretical Trends. *Energy Environ. Sci.* **2015**, *8*, 3022–3029.

(3) Hellstern, T. R.; Benck, J. D.; Kibsgaard, J.; Hahn, C.; Jaramillo, T. F. Engineering Cobalt Phosphide (CoP) Thin Film Catalysts for Enhanced Hydrogen Evolution Activity on Silicon Photocathodes. *Adv. Energy Mater.* **2015**, 1501758.

(4) Laursen, A. B.; Patraju, K. R.; Whitaker, M. J.; Retuerto, M.; Sarkar, T.; Yao, N.; Ramanujachary, K. V.; Greenblatt, M.; Dismukes, G. C. Nanocrystalline Ni5P4 : A Hydrogen Evolution Electrocatalyst of Exceptional Efficiency in Both Alkaline and Acidic Media. *Energy Environ. Sci.* **2015**, *8*, 1027–1034.

(5) Zhen Song; Jan Hrbek, A.; Richard Osgood. Formation of TiO2 Nanoparticles by Reactive-Layer-Assisted Deposition and Characterization by XPS and STM. *Nano Lett.* **2005**, *5*, 1327–1332.

(6) Gross, T.; Ramm, M.; Sonntag, H.; Unger, W.; Weijers, H. M.; Adem, E. H. An XPS Analysis of Different SiO2 Modifications Employing a C 1s as Well as an Au 4f7/2 Static Charge Reference. *Surf. Interface Anal.* **1992**, *18*, 59–64.